Correlated dynamics of water and amphiphilic molecules in thin Newton black films

S. Di Napoli[1,2,a)] and Z. Gamba[1,b)]

[1]*Depto. de Física-GIT-CAC, Comisión Nacional de Energía Atómica, Av. Gral Paz 1499, (1650) San Martín, Buenos Aires, Argentina*
[2]*Consejo Nacional de Investigaciones Científicas y Técnicas, Buenos Aires, Argentina*

The dynamical properties of amphiphilics in Newton black films, as well as those of the water confined between the two charged hydrophilic surfaces, have been calculated *via* a series of molecular dynamic calculations in several films with different water contents. A charged semiflexible amphiphilic model and the TIP5P model of water are used in our simulations [Z. Gamba, J. Chem. Phys. **129**, 164901 (2008)]. We calculate the diffusion coefficients, reorientational dynamics, and the atomic density profile of water molecules as a function of the number of water molecules per amphiphilic (n_w). We also analyze the reorientational motion of the amphiphilics and determine a strong correlation between the dynamics of water molecules and the translational and reorientational dynamics of the amphiphilics, as well as a correlation between the reorientational dynamics of the amphiphilics belonging to the upper and lower halves of the studied thin films. © *2010 American Institute of Physics*. [doi:10.1063/1.3302133]

I. INTRODUCTION

Confined water has been and still is extensively studied due to its mediation in numerous processes that take place in very different environments, such as biological and inorganic membranes, pores, and microemulsions. Under nanoscale confinement, its dynamics and density distributions show large differences with those measured in the bulk.[1–3] Furthermore, the measured differences depend not only on the geometry and size of the cavity but also on the type of confining surfaces, i.e., if they are hydrophobic or hydrophilic.

When water is confined in hydrophobic cavities, it has a weak attractive interaction with the walls, shows large density fluctuations[4] at the interface liquid wall, and therefore exhibits a small friction term as it flows through the hydrophobic cavity of a carbon nanotube,[5] the pores of a biological membrane,[6] or the thin channels analyzed in nanofluidic studies.[7] Molecular dynamics (MD) simulations of these systems also show the absence of an anomaly in the diffusion of water in the direction perpendicular to the hydrophobic wall.[8] Nevertheless, the diffusion is also dependent on the topology of both components, the nanotube[9] and the solute.[10]

On the other hand, when water is confined by hydrophilic surfaces, it has a strong interaction with them and its properties change dramatically. For example, a MD simulation of a thin film of water between two hydrophilic self-assembled monolayers (SAMs) on gold[11] showed that, as the water layer becomes thinner, the diffusion coefficient of water decreases two orders of magnitude with respect to bulk water but, nevertheless, it remains in the liquid state.

A similar phenomenon is found in systems with spherical symmetry. The dynamics of confined water in reverse micelles (the water is in the core of the micelle) of various sizes has been measured by optical techniques by Dokter *et al.*[12] They determined that the surfactant counterions remain near the interface water-surfactant, that water in the interfacial region is much less mobile than in the core of the micelle, and that for large enough micelles, the reorientational dynamics at the core is similar to that of bulk water. Neutron scattering measurements, in small reverse micelles with a radius for water of 7 Å, determine a supercooling of more than 45 K compared to bulk water.[13]

Several calculations that compare the behavior in both types of confinements have been performed. For example, a MD simulation of a water layer (60 Å thick) between two crystalline hydrophobic surfaces have been compared with those obtained in a simulation of the same water layer between two crystalline hydrophilic surfaces.[14] It was determined that the dynamical properties of water are very different: the diffusion parallel to the surfaces is similar to bulk water near the hydrophobic wall and it is reduced about 30% near the crystalline hydrophilic wall. Also MD simulations of thin water layers (with a width of about 2 or 3 water molecules) between two smooth planar walls have determined that, if the confinement is hydrophilic, water does not freeze at low temperatures, but when the confinement is hydrophobic, water freezes into different crystalline structures with no correlation to those of bulk water.[15] Finally, an interesting example of a nanostructure of dual behavior is the hydrated imogolite nanotube that exhibits an external hydrophobic surface while the internal surface is hydrophilic, as determined in Ref. 16.

In this paper we study the properties of water under nanoconfinement in a natural hydrophilic environment, as are the Newton black (NB) films. The disorder and diffusion

---

a)Electronic mail: dinapoli@tandar.cnea.gov.ar.
b)Electronic mail: gamba@tandar.cnea.gov.ar. URL www.tandar.gov.ar/~gamba.

of the charged amphiphilics in these type of bilayers form a hydrophilic wall that has large differences with the much ordered confinement of that determined by two SAMs of neutral amphiphilics on crystalline substrates, as in Ref. 11, or the confinement between two smooth surfaces, as in Ref. 15.

Several simulations of NB films with detailed atomic models of surfactants have been performed since some time ago, mainly to give an insight of the structure and stability of these films: samples of 32 and 64 sodium dodecyl sulfate (SDS) $[CH_3(CH_2)_{11}OSO_3^-Na^+]$ molecules and up to six water molecules per amphiphilics were simulated in Ref. 17, all-atom MD simulations of 32 surfactants (three different series with different surfactants) and up to 1210 water molecules are included in Ref. 18, and finally, in Ref. 19 simulations of 128 SDS and up to 22 water molecules per amphiphilic are presented.

Here we are interested in the dynamical behavior of all type of molecules in these natural bilayers and in their probable intercorrelation. In this type of problems, the small samples of only 32 solvents,[18] although extremely useful to study intramolecular dynamics and solute hydration, could be not enough to study the intermolecular dynamics of amphiphilics and water disordered bilayers. Here we address this problem with a simplified amphiphilic model that nevertheless takes into account the strong electrostatic interactions and the intramolecular amphiphilic modes, by including a charged semiflexible chain model and the TIP5P model of water.[20,21] We present a series of MD simulations of NB films, with increasing width of the water core and analyze the density atomic profile, the amphiphilic translational and reorientational dynamics, the water dipole orientation and diffusion as a function of the water layer width, as well as their possible correlation with the reorientational dynamics and diffusion of the amphiphilics.

II. THE AMPHIPHILIC AND WATER MOLECULE MODELS

The intermolecular potential of water molecules in our MD simulations is described by the classical and rigid molecular model TIP5P.[22,23] It consists of one Lennard-Jones (LJ) site localized at the O atom and four charges. Two positive charges are localized at the H atoms and two negative charges at the lone pairs. This water model gives good results for the calculated energies, diffusion coefficients, and density of water as a function of temperature, including the anomaly in the density near 4 °C and 1 atm.[22] The only reported problem is its failure to reproduce the O–O pair correlation function $g_2(r)$ that locates the first neighbor at a slightly shorter distance than the experimental one;[22] nevertheless, the same problem is reported for an improved potential model consisting of six sites[24] and therefore the TIP5P model of water is selected for our numerical simulations.

Our amphiphilic model corresponds to a simplification of sodium dodecyl sulfate (SDS) $[CH_3(CH_2)_{11}OSO_3^-Na^+]$ in solution. Our negatively charged amphiphilic consists in a semiflexible chain of 14 atoms, in which the bond lengths are held constant but bending and torsional potentials are in-

cluded, in order to simulate the molecular stiffness and to avoid an artificial molecular collapse. The first two atoms of the chain mimic a charged and polar head (atom 1 with a charge of $-2e$, atom 2 with a charge of $1e$), their LJ parameters are: $\sigma_1 = \sigma_2 = 4.0$, $\epsilon_1 = 2.20$ kJ/mol, $\epsilon_2 = 1.80$ kJ/mol. The following 12 uncharged atoms form the hydrophobic tail: sites 3–13 are united atom sites CH_2 and site 14 is the united atom site CH_3. We are also including a Na^+ ion per chain in the MD box. Full details on the molecular geometry, charge distribution, inter- and intramolecular potential parameters are given in Ref. 20 and references therein.

III. THE MODEL BILAYER AND NUMERICAL SIMULATIONS

We performed a series of MD simulations on samples of 256 amphiphilics and increasing the number of water molecules per amphiphilic (n_w) from 1 to 4 (the whole series is of $n_w = 1, 2, 3$ and 4, for $n_w = 2$ we run four different areas per amphiphilic).

The initial configuration, for all samples, is totally similar to that used in Ref. 21. It consists of a preassembled bilayer that was built by arranging half of the chain molecules on a body centered square lattice of 8×8 unit cells, in the (x, y) plane, with lattice constant a. Molecular center of mass of the modeled SDS anions were initially placed at $\left(\frac{1}{4}, 0, \pm z_c\right)$ and $\left(\frac{3}{4}, \frac{1}{2}, \pm z_c\right)$, with the headgroups pointing to the core of the bilayer, which resulted in an initial distance between tail to tail chain layers greater than twice the final measured distance of less than 45 Å in the equilibrated sample. The equilibrated area per amphiphilic, in this paper, is in the range of 17–20 Å².

The MD integration algorithms are identical to those used in our previous simulations of NB films[20,21] and biological membranes.[25] The equations of motion of all molecules are integrated using the velocity Verlet algorithm for the atomic displacements and the SHAKE and RATTLE algorithms for the constant bond length constraints on each molecule. The electrostatic interactions are calculated by using the Ewald's sums for quasibidimensional samples,[20] with a cutoff radius of 12. The time step is 2 fs, the samples are thermalized typically for 20–200 ps, and measured over a free MD trajectory for the following 2 ns (1 ns for the sample with $n_w = 4$). Our MD simulations use the Berendsen algorithm to maintain the constant temperature of the samples.

Figure 1 shows a snapshot of the equilibrated configuration of a NB film, in one of the time steps of a free MD trajectory of 2 ns. This sample consists of 256 charged amphiphilics and 256 Na^+ ions solved in 768 water molecules. The MD box parameters are $a = b = 49.7$ Å, $c = 1000$ Å, and the film width is of about 40 Å, as measured from the average distance between end tails.

IV. RESULTS

A. Density profiles

Figure 2 shows the atomic density profile (number of atoms per Å³, as a function of z) for the samples of 256
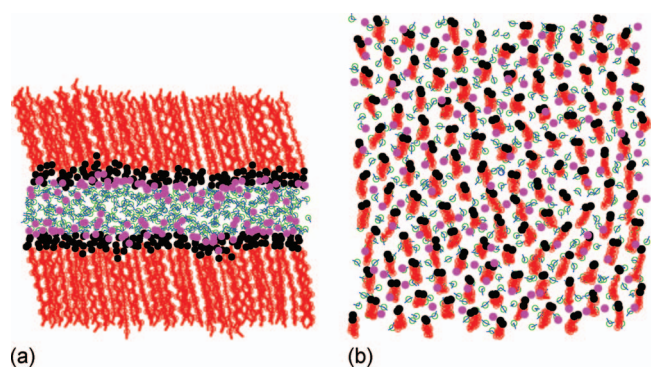
FIG. 1. A snapshot of the equilibrated sample with 256 charged amphiphilics, 256 Na$^+$ ions, and 768 water molecules: (a) *ac* cross section and (b) *ab* cross section. (red: hydrophobic tail, black: polar head, magenta: Na$^+$ ions, and green-blue: water molecules).

amphiphilics, 256 Na$^+$ ions and with $n_w=1,2,3$, and 4 water molecules per amphiphilic. Similar profiles are reported for SDS NB films in Ref. 18, for example.

In Fig. 3 we plotted the water film width ($\Delta_w(z)$) as a function of n_w, it has been measured as the average distance between amphiphilic heads obtained from the atomic density profiles. Figure 3 includes the values from our simulations with 256 chains plus those of 64 chains (obtained from our simulations included in Ref. 21) and 226 chains (from our simulations of Ref. 20). It can be seen that the water film width depends mainly on n_w and in a less extent on the size of the samples, at least for these low values of water content. We locate a discontinuity at $n_w \simeq 1$; for samples with low values of n_w the amphiphilic heads of lower and upper halves of the bilayer interpenetrate and the water surrounds them, forming the hydration layer (although nonbonded, the nearest water molecules reorientate so as to shield the strong electrostatic field of the amphiphilic heads).

A similar behavior was observed also in all-atom MD simulations of 128 molecules of SDS, in a MD box of 33 Å^2 per amphiphilic and $n_w=0-22$, in these films of SDS molecules, the small change in slope was found at $n_w \simeq 2.25$.[19] It
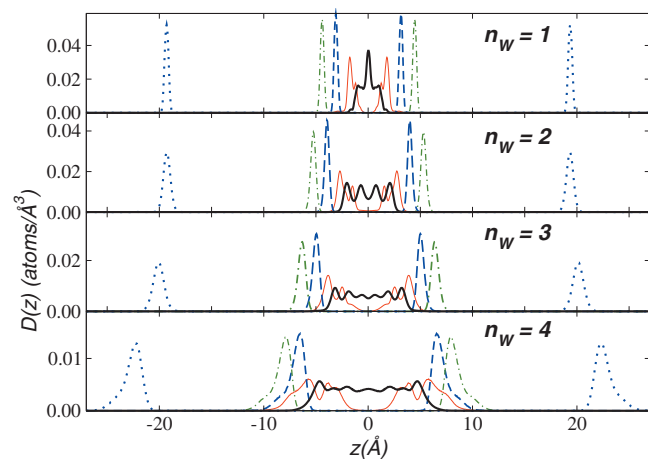

FIG. 2. Atomic density profile (number of atoms per Å^3) for the samples of 256 amphiphilics, 256 Na$^+$ ions, and $n_w=1,2,3$, and 4 water molecules per amphiphilic. $z=0$ at the bilayer core. (dotted blue: tail CH$_3$ of amphiphilics, dashed blue: atom 1 of polar head, point-dashed green: atom 2 of polar head, thin red: Na$^+$ ions, and thick black: O of water molecules).
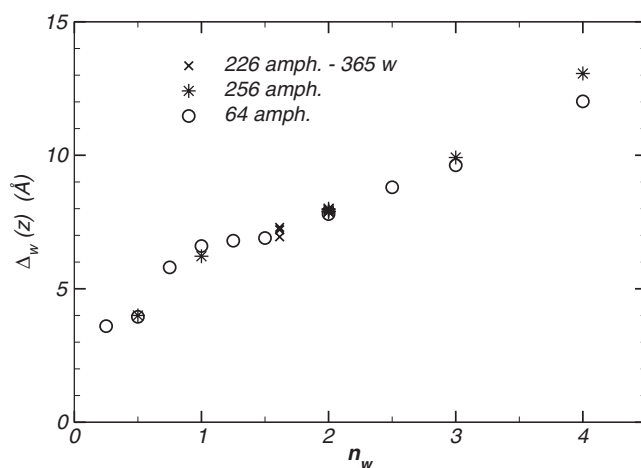

FIG. 3. Water film width as a function of water content per amphiphilic. Errors: smaller than the size of the plotted symbols.

was not detected in Ref. 18, where MD simulations of 32 SDS with a surface concentration of 42.4 Å^2 and $n_w=5.3$ to 32.3, because of the high content of water. It was also not detected in the earlier simulations with 36 and 64 SDS molecules and $n_w=0-6$ (Ref. 17) as in these simulations the change in slope is not clear from the plot of a few points.

B. Translational diffusion

The diffusion coefficients of water and amphiphilics, in the plane of the bilayer, are calculated from the slope at long times of the mean square displacement as a function of time. The averages are performed over all molecules of the same kind and several time origins.

In Table I and Fig. 4 we include the calculated diffusion coefficients for amphiphilics, in our samples of 256 amphiphilics, which range from about $0.1-0.7 \times 10^{-5}$ cm^2/s. The plot shows the slightly trend to increasing values of the diffusion coefficient of amphiphilics as a function of the increasing area per amphiphilic. Table I shows that in these extremely thin films the diffusion of water very closely follows that of the amphiphilics.

With our samples of 256 and 226 (Ref. 20) amphiphilics we obtain considerable lower values of diffusion coefficients than those reported in our Ref. 21 with small samples of 64 amphiphilics. We first attributed this fact to the higher roughness of the two confining surfaces formed by the amphiphilics in our larger samples. Nevertheless, a further calculation of the pair distribution functions of amphiphilic

TABLE I. Calculated diffusion coefficients in the samples of 256 chains. Units: 10^{-5} cm^2/s.

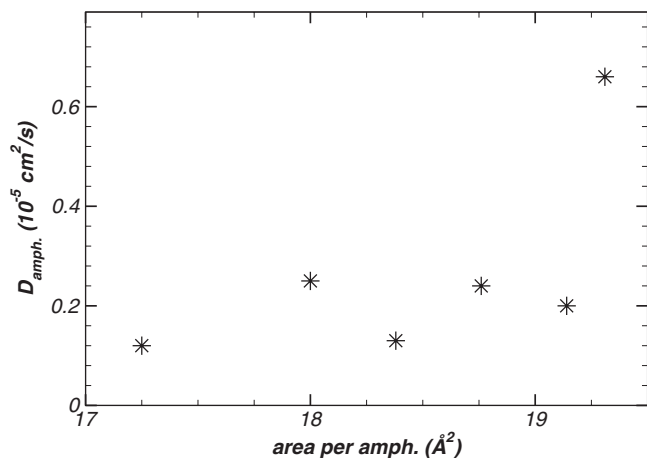| n_w	Area (Å^2)	Amph.	H$_2$O
2	18.00	0.25(1)	0.33(1)
2	18.38	0.13(3)	0.21(1)
2	18.76	0.24(8)	0.33(1)
2	19.14	0.2(1)	0.28(1)
3	19.31	0.66(1)	0.92(1)
4	17.25	0.12(6)	0.26(7)

FIG. 4. Diffusion coefficients for amphiphilics as a function of their effective area. Units: 10^{-5} cm^2/s. Errors: smaller than the size of the plotted symbols.

heads in the **xy** plane (and *xy* snapshots of all samples) shows that they tend to be in a hexagonal crystalline array with dynamic chain reorientation around an axis perpendicular to the bilayer. As our samples are square, the distortion of the hexagonal array is larger for the smaller sample. In our simulations of 64 amphiphilics[21] we found that they not only reorientate around their center of mass, but also jump from one site to other in a much less hindered motion. The reorientational motion of the amphiphilics is included in the following section.

The estimated minimum error in our measurements of the translational diffusion is of about 1×10^{-7} cm^2/s for samples with n_w up to 3; this value is obtained by considering a maximum molecular displacement of about the first neighbor distance during the total time of the measurement (2 ns). For $n_w = 4$, the error is around 2×10^{-7} cm^2/s because the total time of measurement is of 1 ns in this case.

For the sake of comparison, the experimental value of SDS molecules in NB films of about 35 Å thickness is 6×10^{-7} cm^2/s,[26] the experimental diffusion constant of bulk water at STP is $D_w^{exp} = 2.3 \times 10^{-5}$ cm^2/s,[27] and that calculated with the TIP5P model in Ref. 23 is of $D_w = 2.6 \times 10^{-5}$ cm^2/s. For a sample of 500 water molecules at 298 K, using a cutoff radius of 10 Å and Ewald's sums, we obtain a diffusion coefficient of 2.8×10^{-5} cm^2/s.

C. Reorientational diffusion of amphiphilics

In all samples we observe that the amphiphilics show a tilt angle θ with respect to the perpendicular of the bilayer plane (axis z), and that they also perform a collective periodic motion about this axis and around their corresponding center of mass. The time and molecule average value of the z component of a vector that points from the first to the last atom of each amphiphilics gives the cosine of the amphiphilic tilt angle θ. Table II and Fig. 5 clearly show that this tilt angle increases for increasing area per amphiphilic. In this figure we have included the measured values in the samples of 256 amphiphilics and also those obtained in our previously calculated samples of 64 (Ref. 21) and 226 amphiphilics.[20] Errors are about 2°.

TABLE II. Tilt angle and film area per amphiphilic for the samples of 256 amphiphilics.

n_w	θ (deg.)	Area (Å^2)
1	3.3	16.52
2	26.9	18.00
3	29.3	19.31
4	21.6	17.25

In Fig. 6(a) we show an interval of 50 ps of the reorientational motion of the amphiphilics in the plane of the bilayer, for the samples of 256 amphiphilics with tilt angle and area given in Table II. The extremely thin layers of water suggest a further possible correlation between the motion of amphiphilics in the lower and upper halves of the film, and the plot shows that, effectively, they are highly correlated. In this Figure we plotted one of the in-plane component (x) of the oscillatory reorientational motion ($fdx(t)$) for amphiphilics in both layers of the film, averaged on the corresponding number of molecules (N/2),

$$fdx(t) = \frac{2}{N} \sum_{i=1,N/2} d_x^i(t)/d^i(0),$$

where **d** is the in-plane projection of a vector that goes from the first to the last atom of each amphiphilic.

We also calculate the Fourier transform of these components in order to obtain a typical reorientational frequency. In Fig. 6(b) we show that the main frequency of the reorientational motion is the same for amphiphilics in the lower and upper halves of the film. Figure 7 shows, for the sample of 256 chains, $n_w = 2$ and four different values of area per amphiphilic, the close dependence and decreasing value of the typical reorientational frequency with increasing area per amphiphilic. For this particular frequency (ν_p), the amphiphilic motion in upper and lower halves of the bilayer are in counterphase for low values of n_w. As an example, Fig. 8 includes the calculated phase $\phi(\nu)$ for the bilayer with $n_w = 3$. In the sample with $n_w = 4$, the amphiphilic motion is in
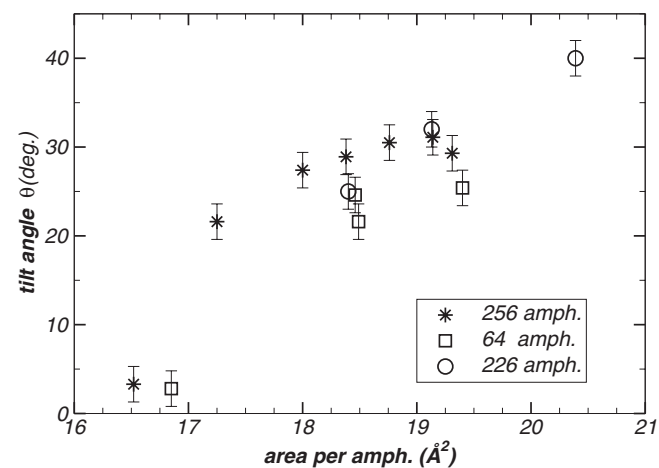

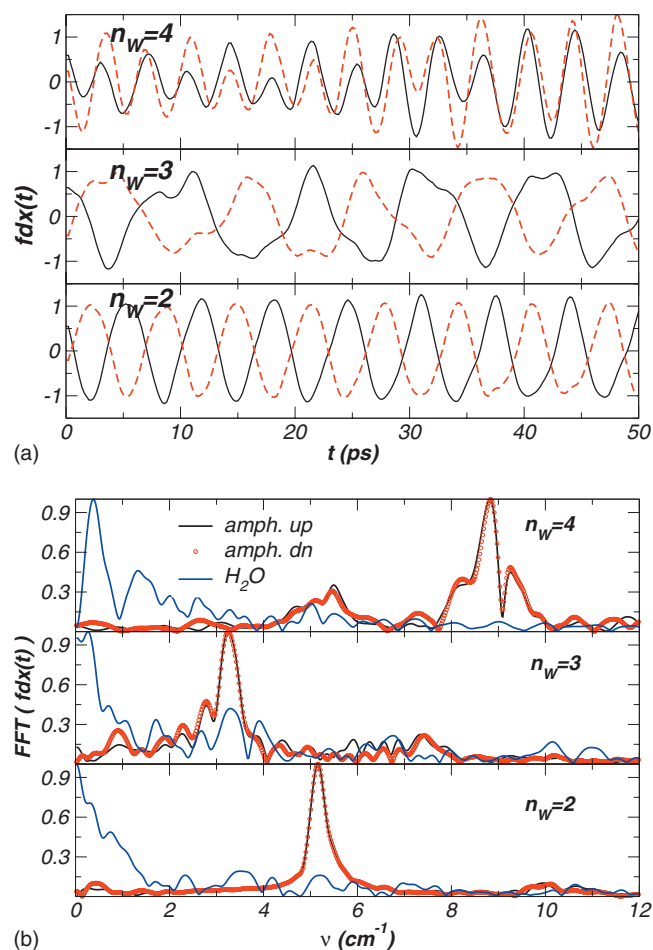FIG. 5. Tilt angle as a function of film area per amphiphilic.

FIG. 6. (a) Projection on the x axis of the reorientational motion in the xy plane, for the amphiphilics in the upper (black) and lower (dashed-red) halves of the bilayers, for $n_w = 2$, 3, and 4 water molecules per amphiphilic. (b) Fourier transform of the amphiphilic and water reorientational motion (upper and lower halves of the bilayer) shown in (a).

phase, although the total dipole moment of the sample, in the plane of the bilayer, is zero when taking into account the amphiphilic and ion charges.

Figure 6(b) also includes the calculated reorientational frequencies for water, calculated in a similar way as that used for amphiphilics, but the vector now refers to the dipole moment of water. The figure shows, for $n_w = 2$ and 3, a nonzero value at the origin that clearly indicates reorientational diffusion for water molecules.

Finally, the decrease in the amphiphilic's typical reorientational frequency ν_p with increasing area [Fig. 7(b)] is closely correlated with the corresponding increase in tilt angle (Fig. 5) and therefore increasing inertia moment around the axis perpendicular to the plane of the bilayer.

D. Reorientational diffusion of water

The reorientational diffusion of water is highly hindered, along the perpendicular to the bilayer plane, by the strong electrostatic field due to ions plus amphiphilics. In Ref. 20 we calculated the macroscopic electrostatic field (along the perpendicular to the bilayer) in NB films of 226 amphiphilics
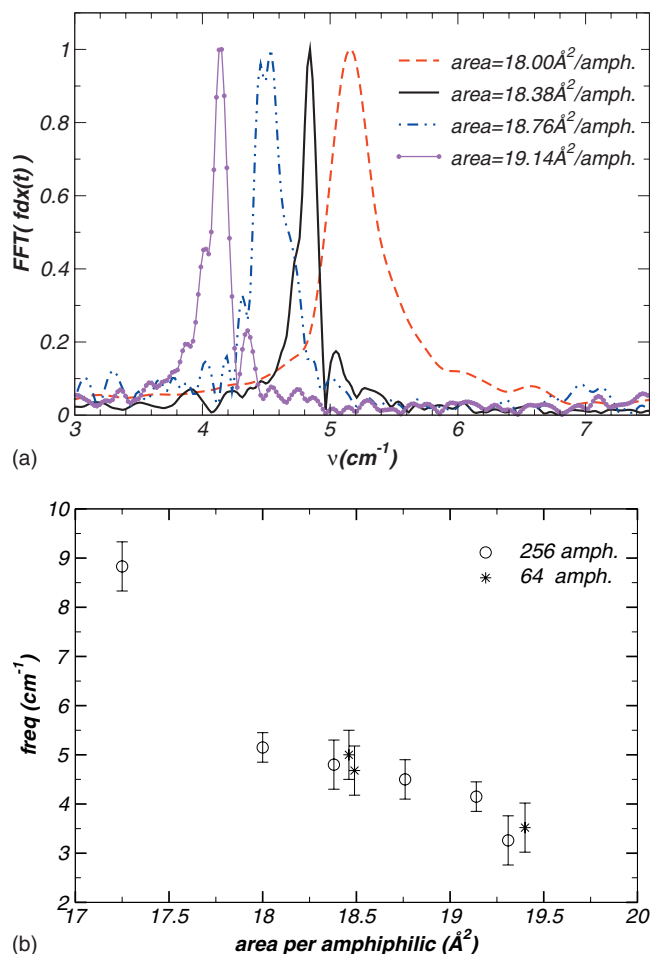
plus 365 water molecules, and showed the strong polarization of water induced by the orientational order of the amphiphilic heads.

In order to obtain the water reorientational characteristic times, we calculated the self-correlation function $C_w^k(t)$, averaged over all water molecules and several time origins, given by

FIG. 7. (a) Typical reorientational frequency of amphiphilics for the sample of 256 amphiphilics, $n_w = 2$, and different values of area per amphiphilic. (b) Reorientational frequencies vs area per amphiphilic.
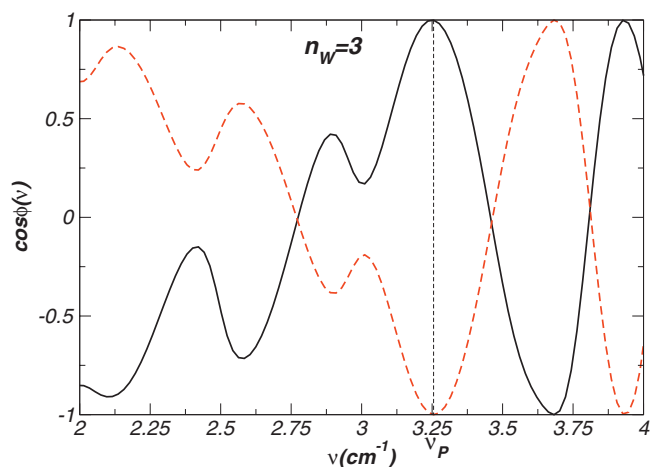

FIG. 8. Measured phase, as a function of frequency, given by the Fourier transform of the reorientational motion of amphiphilics in the sample with $n_w = 3$ of Fig. 6.
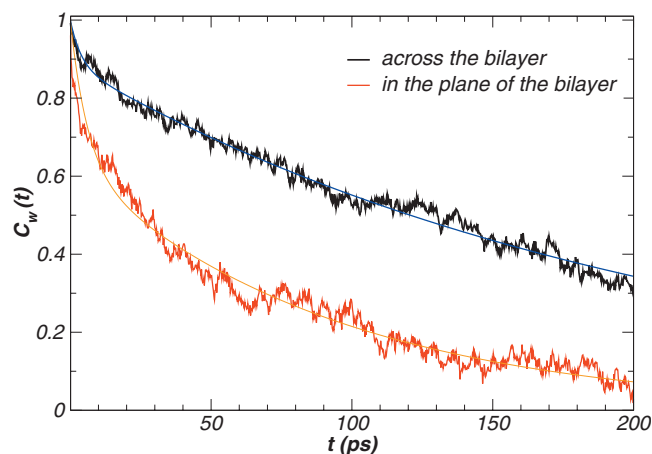
FIG. 9. Reorientational self-correlation functions of water, sample of 256 amphiphilics, 256 ions, and $n_w=3$.

$$C_w^k(t) = \frac{1}{N_w} \sum \mu_i^k(t) \cdot \mu_i^k(0)/\mu_i^k(0)^2,$$

where $\mu_i(t)$ gives the dipole orientation of the water molecule i, k refers to the in-plane (xy) or perpendicular (z) projections, and N_w is the total number of water molecules.

Figure 9 shows a typical decay of the reorientational self-correlation functions for the water dipole, across and within the plane of the bilayer. These functions are calculated as averages over all water molecules and ten time origins. The curves can be fitted by the sum of two exponentials that give the short and long decay times. In Table III we include the calculated reorientational times for the water dipole in four cases. The values are typical for all samples but we could not find a clear correlation between these times and n_w. From the data included in Table III, for $n_w=2$, we can infer that the short decay time (τ_2) is smaller (faster reorientation) for increasing area per amphiphilic. These reorientational times depend not only on the available space for the molecule to reorientate but also on the strength of the local electrostatic field, which in turn, depends on the thickness of the film.
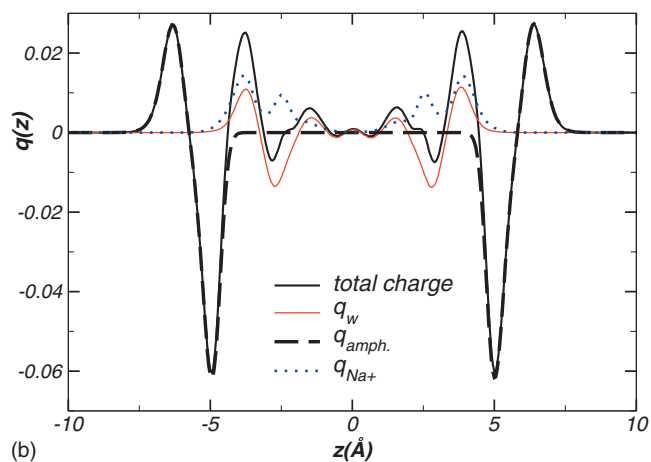
E. Dipolar orientations

The strong electrostatic field generated by the charged heads and ions implies also that the water molecules nearest to the water-lipid interface are strongly polarized along z. Figure 10(a) shows the water polarization (as given by the average water dipole orientation) as a function of z. It can be seen that for increasing values of n_w water becomes less polarized at the core of the bilayer. For the sake of compari-

TABLE III. Calculated decay times for the reorientational motion of the water dipole, for the four samples with $n_w=2$.

Area per amph. (Å^2)	τ_{1z} (ps)	τ_{2z} (ps)	τ_{1xy} (ps)	τ_{2xy} (ps)
18.00	670(200)	24(2)	200(100)	21(2)
18.38	530(100)	29(4)	120(30)	16(3)
18.76	210(30)	4.0(0.5)	90(30)	5(1)
19.14	360(80)	3.7(0.3)	140(40)	5(1)
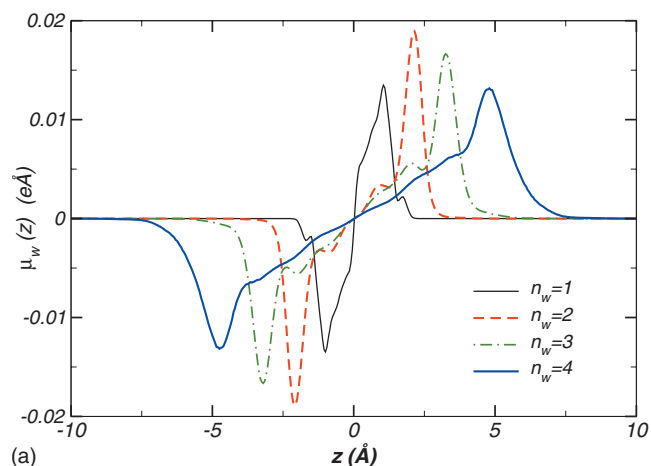
FIG. 10. (a) Average orientation of water dipole along the perpendicular to the bilayer, samples of 256 amphiphilics, and different contents of water. (b) Charge distribution within the bilayer, due to water, ions, and amphiphilics in the sample with $n_w=3$.

son the dipole moment of water is $\mu_w=0.477e$ Å. In Fig. 10(b) we show, as an example, the average total charge distribution within the bilayer for the sample with $n_w=3$ and the separated contribution of water, Na$^+$ ions and amphiphilic heads, as a function of z. The water polarizability and amphiphilic head dipole point outwards, but the charge distribution is such that the total dipole across the bilayer is zero.

The calculated hydration layer determined from Fig. 3 and the strong polarization of water at the water-lipid interface are characteristics of the interaction of water with hydrophilic surfaces.

V. CONCLUSIONS

In this paper we studied the dynamical properties of thin films of water and of their two confining organic hydrophilic surfaces, as exemplified by NB films. We performed a series of MD simulations varying the content of water and using simplified, but nevertheless reliable, intermolecular potential models.[20,21,25] Our simple bilayer model includes amphiphilics with a head that is both charged and polar, a flexible chain tail of 12 sites, including intramolecular bending and torsional potentials (to avoid molecular collapse), Na$^+$ ions, and the TIP5P model for water. The electrostatic interactions are fully taken into account, via Ewald sums in a MD

box with a large empty space (along z), periodic boundary conditions in the xy plane, and a macroscopic electric field term that goes beyond the total dipole moment of the MD box.[20]

Our simple molecular bilayer model includes a full account of electrostatic interactions and thus suggests that reliable and useful conclusions can be obtained from our simulations. Our samples consist of 256 amphiphilics plus ions with up to four water molecules per amphiphilic.

In the calculated range of area per amphiphilic, their center of mass tends to a hexagonal array in the xy plane, showing a tilt angle with respect to the perpendicular of the bilayer plane, and a collective reorientational motion around the same axis. We determined a strong correlation between the reorientational motion of all amphiphilics, even between those in the upper and lower halves of the bilayer, and that a main reorientational frequency can be measured. The main reorientational frequency decreases when increasing the area per amphiphilic, while the translational diffusion and the average amphiphilic tilt angle increase.

The translational diffusion of water follows very closely that of the amphiphilics in this type of extremely thin film, while their reorientational diffusion is highly hindered not only by the available space but also for the strong electrostatic interactions. We measure a strong polarization of water (as given by their average dipole orientation) and a hydration layer, both are typical of water confined by hydrophilic surfaces.

[1] C. A. Angell, Science **319**, 582 (2008).
[2] U. Raviv, P. Laurat, and J. Klein, Nature (London) **413**, 51 (2001).
[3] R. Zangi and A. E. Mark, J. Chem. Phys. **119**, 1694 (2003).
[4] J. Mittal and G. Hummer, Proc. Natl. Acad. Sci. U.S.A. **105**, 20130 (2008).
[5] G. Hummer, Mol. Phys. **105**, 201 (2007).
[6] V. J. van Hijkoop, A. J. Dammers, K. Malec, and M. O. Coppens, J. Chem. Phys. **127**, 085101 (2007).
[7] F. Feuillebois, M. Z. Bazant, and O. I. Vinogradova, Phys. Rev. Lett. **102**, 026001 (2009).
[8] S. Han, P. Kumar, and H. E. Stanley, Phys. Rev. E **77**, 030201(R) (2008).
[9] N. Choudhury, J. Phys. Chem. **112**, 6296 (2008).
[10] Y. Ch. Liu, J. W. Shen, K. E. Gubbins, J. D. Moore, T. Wu, and Q. Wang, Phys. Rev. B **77**, 125438 (2008).
[11] J. M. D. Lane, M. Chandross, M. J. Stevens, and G. S. Grest, Langmuir **24**, 5209 (2008).
[12] A. M. Dokter, S. Woutersen, and H. Bakker, J. Chem. Phys. **126**, 124507 (2007).
[13] T. Spehr, B. Frick, I. Grillo, and B. Stuhn, J. Phys.: Condens. Matter **20**, 104204 (2008).
[14] M. O. Jensen, O. G. Mouritsen, and G. H. Peters, J. Chem. Phys. **120**, 9729 (2004).
[15] P. Kumar, F. W. Starr, S. V. Buldyrev, and H. E. Stanley, Phys. Rev. E **75**, 011202 (2007).
[16] B. Creton, D. Bougeard, K. Smirnov, J. Guilment, and O. Poncelet, Phys. Chem. Chem. Phys. **10**, 4879 (2008).
[17] Z. Gamba, J. Hautman, J. C. Shelley, and M. L. Klein, Langmuir **8**, 3155 (1992).
[18] S. S. Jang and W. A. Goddard III, J. Phys. Chem. B **110**, 7992 (2006).
[19] F. Bresme and J. Faraudo, Langmuir **20**, 5127 (2004).
[20] Z. Gamba, J. Chem. Phys. **129**, 164901 (2008).
[21] S. Di Napoli and Z. Gamba, Physica B **404**, 2883 (2009); number dedicated to the meeting "Frontiers in Condensed Matter" held in Buenos Aires, Argentina, December 2008.
[22] M. W. Mahoney and W. L. Jorgensen, J. Chem. Phys. **112**, 8910 (2000).
[23] M. W. Mahoney and W. L. Jorgensen, J. Chem. Phys. **114**, 363 (2001).
[24] H. Nada and J. P. J. M. van der Eerden, J. Chem. Phys. **118**, 7401 (2003).
[25] Z. Gamba, J. Chem. Phys. **129**, 215104 (2008).
[26] D. C. Clark, R. Dann, A. R. Mackie, J. Mingins, A. C. Pinder, P. W. Purdy, E. J. Russel, L. J. Smith, and D. R. Wilson, J. Colloid Interface Sci. **138**, 195 (1990).
[27] R. Mills, J. Phys. Chem. **77**, 685 (1973).